This article was downloaded by: [University of California, San Diego]
On: 08 August 2012, At: 14:20
Publisher: Taylor & Francis
Informa Ltd Registered in England and Wales Registered Number: 1072954
Registered office: Mortimer House, 37-41 Mortimer Street, London W1T 3JH, UK

Molecular Crystals and Liquid Crystals

Publication details, including instructions for authors and subscription information:
http://www.tandfonline.com/loi/gmcl20

Flexoelectricity in Electroconvection

T. Tóth-Katona [a], N. Éber [a] & Á. Buka [a]

[a] Research Institute for Solid State Physics and Optics, Hungarian Academy of Sciences, Budapest, Hungary

Version of record first published: 05 Oct 2009

To cite this article: T. Tóth-Katona, N. Éber & Á. Buka (2009): Flexoelectricity in Electroconvection, Molecular Crystals and Liquid Crystals, 511:1, 11/[1481]-24/[1494]

To link to this article: http://dx.doi.org/10.1080/15421400903048461

PLEASE SCROLL DOWN FOR ARTICLE

Full terms and conditions of use: http://www.tandfonline.com/page/terms-and-conditions

This article may be used for research, teaching, and private study purposes. Any substantial or systematic reproduction, redistribution, reselling, loan, sub-licensing, systematic supply, or distribution in any form to anyone is expressly forbidden.

The publisher does not give any warranty express or implied or make any representation that the contents will be complete or accurate or up to date. The accuracy of any instructions, formulae, and drug doses should be independently verified with primary sources. The publisher shall not be liable for any loss, actions, claims, proceedings, demand, or costs or damages

whatsoever or howsoever caused arising directly or indirectly in connection with or arising out of the use of this material.

Downloaded by [University of California, San Diego] at 14:20 08 August 2012

Mol. Cryst. Liq. Cryst., Vol. 511, pp. 11/[1481]–24/[1494], 2009
Copyright © Taylor & Francis Group, LLC
ISSN: 1542-1406 print/1563-5287 online
DOI: 10.1080/15421400903048461

Taylor & Francis
Taylor & Francis Group

Flexoelectricity in Electroconvection

T. Tóth-Katona, N. Éber, and Á. Buka
Research Institute for Solid State Physics and Optics, Hungarian Academy of Sciences, Budapest, Hungary

We reexamine the influence of the flexoelectricity on the electroconvection (EC), the effect which has previously been studied in the conductive EC regime only. Now we extend our studies to the dielectric EC, and to the parameter range for which the standard model of EC excludes the existence of the instability. First, we demonstrate that inclusion of flexoelectricity into the standard model of EC provides a finite EC threshold even for this "forbidden" material parameter range (in accordance with the experiments). Second, we show that flexoelectricity considerably decreases the threshold voltage for the dielectric regime. Finally, we present a novel frequency dependence of the threshold voltage for all EC patterns in the case when the period of the driving frequency becomes comparable with the director relaxation time.

Keywords: electroconvection; flexoelectricity; pattern formation

Downloaded by [University of California, San Diego] at 14:20 08 August 2012

INTRODUCTION

Incorporation of the flexoelectric polarization into the nematohydrodynamic equations [1] produces an additional contribution to the charge distribution and to the electric torque acting on the director. Nevertheless, it has been shown almost two decades ago that in the conductive regime of electroconvection (EC) flexoelectricity affects only slightly the threshold voltage and the wave-number of the patterns [2,3]. The inclusion of flexoelectricity yields only a considerable change in

The authors thank to W. Pesch and A. Krekhov for helpful discussions and for providing the numerical code. Financial supports by the Hungarian Research Fund OTKA-K61075 and by the HAS-KOSEF Bilateral Scientific Exchange Program are gratefully acknowledged.

Address correspondence to Á. Buka, Research Institute for Solid State Physics and Optics, Hungarian Academy of Sciences, P.O. 49, H-1525 Budapest, Hungary. E-mail: ab@szfki.hu

the direction of the wave-vector. Flexoelectricity is characterized by the splay and bend flexoelectric coefficients [4], e_1 and e_3, that are not easy to measure, moreover, data obtained by different methods vary considerably. For these reasons, the flexoelectric polarization has typically been neglected in the theoretical analysis of EC. Measurements on a number of nematics agree, however, that $\sim 10\,\mathrm{pC/m}$ is established as a typical order of magnitude for both e_1 and e_3 [5].

The standard model (SM) of electroconvection [6] excludes the existence of EC patterns in nematics with parameter combination $\varepsilon_a < 0$, $\sigma_a < 0$ ($\varepsilon_a = \varepsilon_\parallel - \varepsilon_\perp$ is the dielectric anisotropy and $\sigma_a = \sigma_\parallel - \sigma_\perp$ is the electric conductivity anisotropy, $\parallel$ denotes the value along, $\perp$ perpendicular to the director $\mathbf{n}$). Nevertheless, EC patterns have been observed in such compounds long ago [7] and have been reconsidered systematically recently in a few nematics [8–10]. Since the observed patterns are not captured by the SM, the instability has been coined as nonstandard EC (ns-EC) [8]. Some characteristics of these patterns, especially the orientation of the rolls (which is parallel with the initial director, similarly to the non-convective, flexoelectricity triggered, striped pattern observed at dc driving [11]) already suggest a possible important role of flexoelectricity in the ns-EC mechanism.

Previous analysis of the SM, which concluded in a minor role of flexoelectricity [2,3] in EC, have been restricted to the conductive regime in samples having typical thickness of $d \geq 10\,\mu\mathrm{m}$. The influence of the flexoelectricity on the dielectric regime has remained an open issue, which we will also discuss here.

In addition, we show experimentally and numerically that the role of the flexoelectricity in EC is also crucial when the period of the driving frequency $1/f$ becomes comparable with one of the characteristic times of the system, namely, the director relaxation time τ_d.

EXPERIMENTAL AND NUMERICAL DETAILS

Our measurements have been carried out on the one hand using commercial nematics Phase 5, Phase 5A, and Phase 4 (from Merck & Co., Inc.), as well as 4-methoxy-benzylidene-4′-n-butyl-aniline (MBBA). All these nematics have $\varepsilon_a < 0$ and $\sigma_a > 0$, i.e., they exhibit "standard" EC (s-EC) at and above a threshold voltage U_c, which is well described by the SM. On the other hand, experiments have also been made on the compound 4-n-octyloxy-phenyl-4-n′-heptyloxy-benzoate (**8**/**7**), which has $\varepsilon_a < 0$ over the whole nematic range, but shows a sign inversion from $\sigma_a < 0$ to $\sigma_a > 0$ as the temperature is increased toward the clearing point. Consequently, in this compound both ns-EC and s-EC could be investigated (although at different temperatures).

Downloaded by [University of California, San Diego] at 14:20 08 August 2012

Samples in the thickness range from $d \approx 3\,\mu m$ to $d = 40\,\mu m$ have been prepared from glass plates coated with etched ITO electrodes and with rubbed polyimide layer (to ensure planar alignment). The cells have been placed into an Instec hot-stage thermostatted within $\pm 0.05^{\circ}C$. EC patterns have been studied with polarizing microscopy using either the shadowgraph technique or two crossed (or nearly crossed) polarizers. The images have been recorded with a digital camera.

For the numerical calculations the "extended SM" (with flexoelectricity included) [12] has been used which concludes to six coupled PDEs for the director components, flow velocities and the electric potential. These PDEs have been listed as equations A6 – A11 in Ref. [12]. Inclusion of the flexoelectric polarization into the nematohydrodynamic equations establishes a coupling between the conductive (charge distribution oscillates with f and the director field is stationary in leading order) and dielectric (director field oscillates with f and the charge distribution is stationary in leading order) modes resulting in a complex time dependence. The solutions still can be classified according to their spatiotemporal parity [12]: the even parity solution corresponds to the conductive regime, while the odd parity solution represents the dielectric regime. Linear stability analysis has been carried out as previously described [12] to obtain the onset behavior. The growth rates for spatial fluctuations have been calculated as a function of the applied voltage. The minimum of the neutral surface (where the growth rate is zero) provided the threshold voltage U_c. At the bounding plates strong anchoring of the director and no slip condition for the flow have been assured by a Galerkin method. The field variables have been expanded into sets of functions that vanish at the boundaries and the time periodicity has been ensured by a Fourier expansion. In the calculations experimentally measured sets of material parameters (permittivities, conductivities, elastic moduli, viscosities) have been used (see Table 1 of [13] for Phase 5 and MBBA, and the Appendix of [12] for **8**/**7**). The flexoelectric coefficients e_1 and e_3 served as fitting parameters (within a reasonable range of values posed by flexoelectric measurements on several nematics compounds [5]).

NON-STANDARD ELECTROCONVECTION

First, we summarize the main features of the ns-EC patterns detected in **8**/**7** at the onset of instability in the temperature range where $\sigma_a < 0$. In a polarizing microscope with crossed (or nearly crossed) polarizers they appear in the form of colored stripes. One can immediately perceive several differences compared to the s-EC patterns. The ns-EC structure becomes invisible when one polarizer is removed, i.e.,

Downloaded by [University of California, San Diego] at 14:20 08 August 2012

it does not produce a shadowgraph image in contrast to the s-EC. The orientation of the ns-EC stripes is parallel (or nearly parallel) with the initial director **n**, contrary to the normal or slightly oblique rolls of s-EC. The ns-EC pattern is quite weak, the overall contrast is much lower than that of the s-EC structure. On the other hand, the ns-EC stripe pattern is remarkably stable over a wide voltage range. In terms of the dimensionless voltage $\xi = (U/U_c)^2 - 1$, the developing ns-EC pattern remains stable up to $\xi \approx 2$, while in s-EC secondary instabilities and even turbulence can develop already at much lower ξ (≈ 0.1).

The threshold voltage U_c for ns-EC scales linearly with the sample thickness d, i.e., the instability is characterized by a threshold electric field (similarly to the dielectric s-EC) instead of a threshold voltage (as in conductive s-EC). U_c increases with the driving frequency f almost linearly which is again different from the situation in s-EC, where the $U_c(f)$ curve either grows rapidly approaching the crossover frequency f_c (the upper frequency limit of the conductive s-EC), or exhibits an $U_c \propto (f)^{1/2}$ dependence (in the dielectric s-EC).

The dimensionless wave number $q_c = 2d/\lambda$ (λ – wavelength of the pattern) in general increases with f [9], and it also increases with the increase of d (but q_c and d are not proportional). This $q_c(d)$ dependence in the ns-EC is again different from that in the s-EC, where, in the conductive regime $\lambda \propto d$ (i.e., $q_c = \text{const}$), while in the dielectric regime of s-EC $\lambda = \text{const}$ (i.e., $q_c \propto d$).

The SM (without flexoelectricity) can not explain the phenomena described above since, as already mentioned, it excludes the existence of electroconvection in nematics with the parameter combination $\varepsilon_a < 0$, $\sigma_a < 0$. Namely, the linear stability test does not allow for any pattern (there is no finite instability threshold) in the whole (physically reasonable) frequency range.

The orientation of the ns-EC stripes (parallel or nearly parallel with ***n***) shows a great similarity to the so-called flexoelectric domains which have been observed long ago [14] at dc and at very low frequency ac driving, and been explained as static, convection free director deformation of flexoelectric origin. This suggests that flexoelectricity may play an important role in the ns-EC mechanism.

Incorporating the flexoelectric polarization into the SM (extended SM) has indeed led to a finite EC threshold for a pattern with dielectric time symmetry and with high roll obliqueness [12] for $\varepsilon_a < 0$ and $\sigma_a < 0$. We mention here that the dielectric character of the ns-EC patterns has also been confirmed by light diffraction measurements [15].

In Figure 1 we confront experimental frequency dependencies of U_c and q_c (bullets and squares, respectively) in a relatively thick ($d = 40\,\mu\text{m}$) sample of **8**/**7** with the results of numerical calculations

Downloaded by [University of California, San Diego] at 14:20 08 August 2012

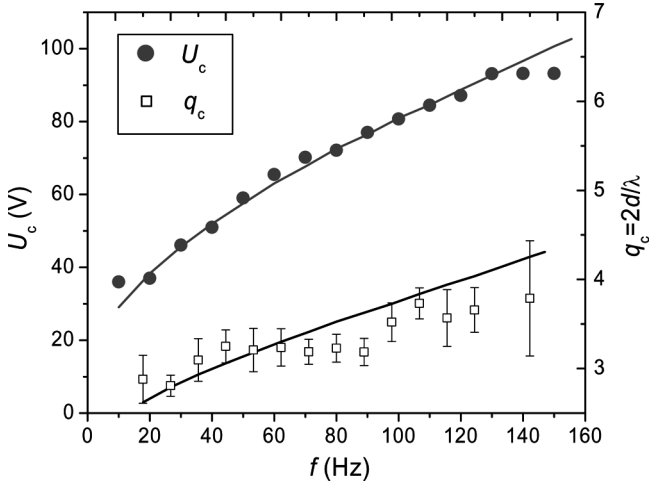

FIGURE 1 Measured frequency dependence of the critical voltage U_c (bullets) and of the modulus of the critical wave-vector q_c (squares) in the nonstandard EC regime for the nematic **8**/**7** in a $d = 40\,\mu m$ sample at $T = 86°C$. The lines represent the result of the numerical calculations.

based on the extended SM (lines). The fitting procedure with $e_1 = -28.3\,pC/m$ and $e_3 = -31.2\,pC/m$ gave a quite good match between the experiments and the theory. Moreover, the roll angle α between $\boldsymbol{q_c}$ and **n** has been found practically frequency independent both in the experiments ($\alpha \approx 75°$) and in the calculations ($\alpha \approx 65°$). This is again an acceptable agreement, especially taking into account that besides the lower contrast, the ns-EC patterns have been found in the experiments less regular at onset than the typical s-EC ones which is manifested in the spatial variation of the wavelength λ (see the relatively large error bars for q_c in Fig. 1) as well as of the orientation of the stripes. It presumably results from a shallower neutral surface [1] (i.e., broader wave-number band) compared to s-EC.

Finally, we mention that a comparison between the experiments and the theory becomes more difficult in thinner ($d \leq 10\,\mu m$) samples where a competition of the characteristic time scales of EC occurs and where the flexoelectricity introduces additional complications. This situation will be discussed in a separate section.

DIELECTRIC EC AND FLEXOELECTRICITY

Now we turn to the most common case of s-EC ($\varepsilon_a < 0$, $\sigma_a > 0$, planar geometry) and focus on the influence of flexoelectricity on the onset

Downloaded by [University of California, San Diego] at 14:20 08 August 2012

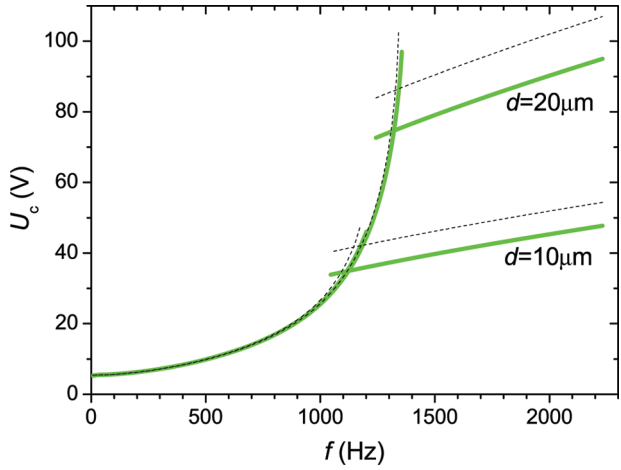

FIGURE 2 Calculated frequency dependence of the critical voltage U_c with and without flexoelectricity (solid and dashed lines, respectively) for the nematic Phase 5 with $d = 10\,\mu m$ and $d = 20\,\mu m$.

characteristics. In Figure 2 the calculated frequency dependence of the threshold voltage U_c is presented for Phase 5 with $\sigma_\perp = 8.2 \cdot 10^{-8}$ $(\Omega m)^{-1}$ at two different thicknesses ($d = 10\,\mu m$ and $d = 20\,\mu m$), both with flexoelectric polarization ($e_1 = -26.5\,pC/m$ and $e_3 = -23.6\,pC/m$, solid lines) and without flexoelectricity ($e_1 = e_3 = 0$, dashed lines). The above values of e_1 and e_3 have been obtained from fits to experimental points that will be presented in the next Section. As one sees, the crossover frequency f_c that divides the conductive and the dielectric regime of s-EC shifts towards lower frequencies when d is decreased, primarily because the dielectric EC threshold becomes lower. Below f_c, in the conductive regime the $U_c(f)$ curves (with and without flexoelectricity) practically coincide (except at very low frequencies, that will be discussed in the next Section). Moreover, no significant change in q_c is caused by the flexoelectric polarization. Therefore, earlier results [2,3] stating that flexoelectricity does not affect considerably the threshold voltage and the wave-number of the conductive s-EC patterns are reaffirmed.

Above f_c, in the dielectric regime, however, flexoelectricity decreases the threshold voltage considerably (by about 10 to 20%, depending on d and on $\sigma_\perp$). In the same time, flexoelectric polarization increases q_c (again by about 10 to 20%) compared to the case of $e_1 = e_3 = 0$, and introduces a nonzero α, i.e., results in dielectric oblique rolls. Therefore, the effect of the flexoelectric polarization can not be

Downloaded by [University of California, San Diego] at 14:20 08 August 2012

disregarded when the threshold characteristics of the dielectric s-EC are investigated.

FLEXOELECTRICITY AND COMPETING TIME SCALES IN EC

In the EC mechanism described by the SM one can distinguish three characteristic time scales: the director relaxation time $\tau_d = (\gamma_1 d^2)/(K_{11}\pi^2)$ (γ_1 – rotational viscosity, K_{11} – splay elastic modulus), the charge relaxation time $\tau_q = \varepsilon_0 \varepsilon_\perp / \sigma_\perp$ (ε_0 – permittivity of free space) and the viscous relaxation time $\tau_v = \rho d^2/(\alpha_4/2)$ (ρ – density, $\alpha_4/2$ – isotropic viscosity). One may expect some peculiarities in the EC mechanism when these relaxation times are approached with the period $1/f$ of the driving frequency. Under common experimental conditions [$d \sim 10\,\mu$m, $\sigma_\perp \sim 10^{-8}$ $(\Omega m)^{-1}$], $\tau_d \sim 1$–10 s, $\tau_q \sim 10^{-3}$–10^{-4} s and $\tau_v \sim 10^{-5}$ s, while the period of the driving frequency in typical EC measurements is mostly in the range $10^{-3}\,\text{s} < 1/f < 0.1\,\text{s}$. At lower frequencies (i.e., for $1/f > 0.1$ s) the determination of U_c may become problematic (the EC pattern obtains a transient character). On the other hand, at higher frequencies (i.e., $1/f < 10^{-3}$ s) the EC pattern may become spatially inhomogeneous, U_c is usually high, q_c is typically small, and therefore, this high frequency range is generally avoided in the measurements.

It might be an easier way to study the problem of matching time scales, if the values of $1/\tau_d$, $1/\tau_q$ and $1/\tau_v$ are brought into a frequency range where EC patterns can conveniently be studied. On the one hand, $1/\tau_d$ can be shifted to higher frequencies by decreasing d down to a few microns, and $1/\tau_q$ can be lowered using low conductivity $\sigma_\perp$. On the other hand, the decrease of $1/\tau_v$ to say $\sim$100 Hz would require extremely thick samples ($d \sim 1$ mm) which would raise other experimental difficulties (initial alignment, visibility of the pattern, etc.). Here, we mainly focus on tuning τ_d with d.

In the main plot of Figure 3 the frequency dependence of U_c is presented for a d=$(3.4 \pm 0.5)\mu$m sample of Phase 5 with $\sigma_\perp = 8.2 \cdot 10^{-8}$ $(\Omega m)^{-1}$. In this case $1/\tau_d \approx 60$ Hz, $1/\tau_q \approx 1800$ Hz, and $1/\tau_v \approx 210^6$ Hz. In the measurements *conductive* s-EC (open circles) has been detected at onset below $f_c \approx 550$ Hz in the form of traveling oblique rolls and traveling normal rolls. Above f_c traveling dielectric rolls (bullets) have been observed. A novel feature of the conductive $U_c(f)$ can be seen at low frequencies (below 100 Hz, in the vicinity of $1/\tau_d$): the threshold decreases by lowering the frequency, i.e., the $U_c(f)$ "bends down". This property has remained undetected in previous studies performed on thicker ($d \geq 10\,\mu$m) samples. In Figure 3 results of numerical calculations both with and without flexoelectric polarization are also presented (solid lines and dashed lines, respectively).

Downloaded by [University of California, San Diego] at 14:20 08 August 2012

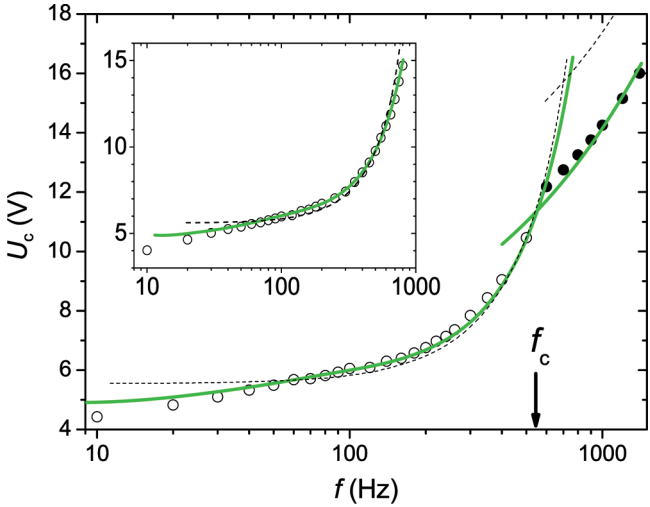

FIGURE 3 Frequency dependence of the EC threshold voltage U_c in a $d = (3.4 \pm 0.5)\,\mu m$ sample of Phase 5 with $\sigma_\perp = 8.2 \times 10^{-8}\,(\Omega m)^{-1}$ – conductive EC (circles), and dielectric EC (bullets). The solid and dashed lines are the results of the numerical analysis with and without the flexoelectric effect, respectively. The arrow indicates the crossover frequency f_c. Inset: the frequency dependence of U_c in the conductive regime of EC for a $d = (3.1 \pm 0.5)\,\mu m$ sample of Phase 5A with $\sigma_\perp = 9.2 \times 10^{-8}\,(\Omega m)^{-1}$.

Calculations without flexoelectricity do not reproduce the "bending down" of $U_c(f)$ at low frequencies in contrast to the case when the flexoelectric polarization is included. With $e_1 = -26.5 pC/m$ and $e_3 = -23.6\,pC/m$ a good match has been obtained with the experimental data in the whole frequency range (including the low f region). Note that above f_c the flexoelectric polarization reduces the dielectric EC threshold noticeably (as discussed in the previous Section) and brings together the theoretical curve with the experimental data.

Control measurements of $U_c(f)$ have also been made on a $d = (3.1 \pm 0.5)\,\mu m$ sample of Phase 5A with $\sigma_\perp = 9.2 \cdot 10^{-8}\,(\Omega m)^{-1}$. Results obtained for the conductive regime are presented in the inset of Figure 3 (open circles) and one can immediately notice that $U_c(f)$ "bends down" in the vicinity of $1/\tau_d$ similarly to the case of Phase 5. Phase 5A has the same chemical composition as Phase 5 just it is doped with ionic salt in order to increase the electric conductivity. Therefore, in the numerical calculations for Phase 5A the material parameters of Phase 5 have been used (including e_1 and e_3). Results of these calculations both with and without flexoelectricity are also

Downloaded by [University of California, San Diego] at 14:20 08 August 2012

presented in the inset of Figure 3 (solid and dashed lines, respectively). The simulated $U_c(f)$ curve with $e_1 = -26.5\text{pC/m}$ and $e_3 = -23.6\,\text{pC/m}$ is in quantitative agreement with the experimental data, contrary to the one without flexoelectricity that does not exhibit the "bending down" at low frequencies, and which also deviates significantly from the measurements at high frequencies.

The main difference between the $U_c(f)$ curves calculated with and without flexoelectricity is that the curvature changes sign [$U_c(f)$ has an inflection point] when flexoelectricity is included, indicating that at high frequencies the flexoelectric contribution to the charge separation becomes negligible compared to the Coulomb one. It is convenient to use the location of the inflection point, f_{infl}, as a quantitative measure. We note here that naturally f_{infl} is slightly higher than the frequency where the bending down becomes obvious. For example, in the main plot of Figure 3 $f_{\text{infl}} = 110\,\text{Hz}$, while the "bending down" becomes unambiguous for $f < 100\,\text{Hz}$. Interestingly, f_{infl} has been found proportional to d^{-1} as it is shown in Figure 4, in contrast to the d^{-2} dependence of $1/\tau_d$. Figure 4 also indicates that an inflection point in $U_c(f)$ does exist even in thicker samples (with large τ_d), however, then the "bending down" is shifted to much lower frequencies (below 10 Hz). Presumably that is the reason why this novel feature of $U_c(f)$ remained unnoticed in previous measurements and calculations.

The crossover frequency f_c shifts to lower values with the reduction of d and/or $\sigma_\perp$. When both d and $\sigma_\perp$ are small enough, the conductive

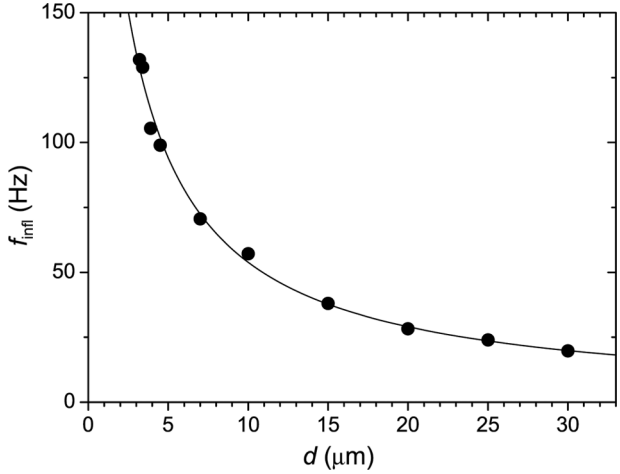

FIGURE 4 Calculated thickness dependence of f_{infl} for Phase 5 with $\sigma_\perp = 8.2 \times 10^{-8}\,(\Omega\text{m})^{-1}$. The solid line corresponds to a linear ${f_{\text{infl}}}^{-1}(d)$ fit.

Downloaded by [University of California, San Diego] at 14:20 08 August 2012

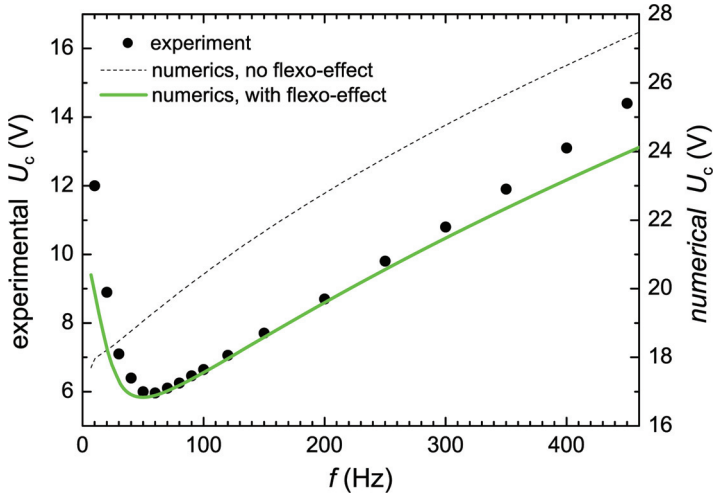

FIGURE 5 Frequency dependence of the dielectric EC threshold voltage U_c measured in a $d = (3.4 \pm 0.5)\,\mu m$ sample of Phase 5 with $\sigma_\perp = 1 \times 10^{-8}\,(\Omega m)^{-1}$ (bullets). The solid and dashed lines are the threshold curves calculated with Phase 5 parameters (except $\sigma_a/\sigma_\perp = 0.1$) with and without the flexoelectric effect, respectively.

regime does not occur at all. Instead, *dielectric* s-EC is observed in the whole frequency range as illustrated in Figure 5, where the frequency dependence of U_c is presented (bullets) for a $d = (3.4 \pm 0.5)\,\mu m$ sample of Phase 5 with $\sigma_\perp = 110^{-8}\,(\Omega m)^{-1}$ ($1/\tau_d \approx 60\,Hz$, $1/\tau_q \approx 220\,Hz$, $1/\tau_v \approx 2 \cdot 10^6\,Hz$). If one considers that both the SM and previous experiments have provided a square root-like $U_c(f)$, the dependence in Figure 5 is rather surprising. Here, $U_c(f)$ "bends up" as $f \to 0$, resulting in a non-monotonic function with an expressed minimum f_{min} in the vicinity of $1/\tau_d$. Above f_{min}, $U_c(f)$ is linear within the experimental error. Similar results have been found for dielectric EC in a $d = (3.2 \pm 0.5)\,\mu m$ sample of Phase 4.

Unfortunately, simulations based on the "extended" SM (i.e., flexoelectricity included) with Phase 5 parameters could not reproduce the experimental results. The calculated threshold curve $U_c(f)$ has been found monotonic (square root-like) with thresholds lower than the experimental values. However, a *qualitative* match to the experimental behavior has been found in the frame of the "extended" SM just by lowering the electric conductivity anisotropy to $\sigma_a/\sigma_\perp = 0.1$ as shown in Figure 5 with solid line. Note that the calculated curve has a minimum at about the same f_{min} frequency where the experimental data,

Downloaded by [University of California, San Diego] at 14:20 08 August 2012

Downloaded by [University of California, San Diego] at 14:20 08 August 2012

and the steepness dU_c/df reproduces the experiments. However, the calculated values of U_c are higher than in the measurements. To demonstrate the role of flexoelectricity in the "bending up" of the $U_c(f)$, in Figure 5 we also plot the results of calculations based on the SM (without the flexoelectric polarization) with the same $\sigma_a/\sigma_\perp = 0.1$ (dashed line). As one sees, $U_c(f)$ is a monotonically increasing function without a minimum. Therefore, the bending up is undisputedly attributed to flexoelectricity, and f_{min} indicates the frequency range where the crossover between dominantly flexoelectric and dominantly Coulomb charge separation mechanisms occurs.

Systematic calculations at $\sigma_a/\sigma_\perp = 0.1$ and $\sigma_\perp = 110^{-8}(\Omega m)^{-1}$ (i.e., $\tau_q = \text{const}$) have shown that with the decrease of d (i.e., of τ_d) f_{min} shifts to higher frequencies. The values of $f_{min}(d)$ have been found close to $1/\tau_d(d)$ as it is illustrated in Figure 6.

Finally, we switch back to the *nonstandard EC* observed in **8**/**7**. As already mentioned, in relatively thick ($d \geq 10\,\mu m$) samples the frequency dependence of U_c is close to linear as it is illustrated in Figure 7 for $d = 13.2\,\mu m$. However, this situation changes when d is decreased (i.e., $1/\tau_d$ is increased) and $U_c(f)$ becomes non-monotonic with a minimum at f_{min} – see results for $d = 3.4\,\mu m$ and $d = 2.4\,\mu m$ in Figure 7. While f_{min} grows, dU_c/df (above f_{min}) decreases with lowering d – these are the same properties that have been found for

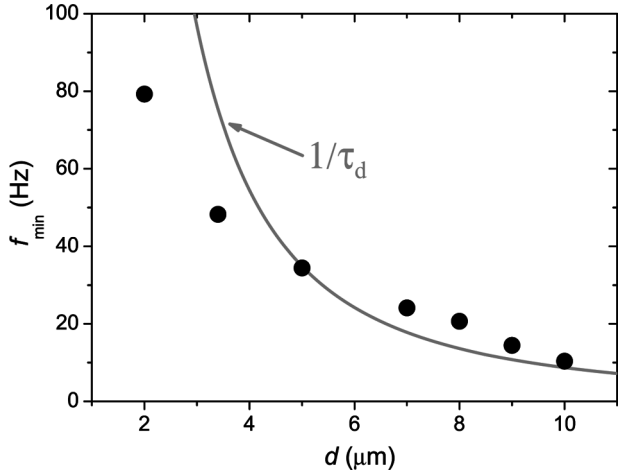

FIGURE 6 Calculated thickness dependence of f_{min} for Phase 5 with $\sigma_\perp = 1 \times 10^{-8}(\Omega m)^{-1}$ and $\sigma_a/\sigma_\perp = 0.1$. The solid line is the thickness dependence of $1/\tau_d$.

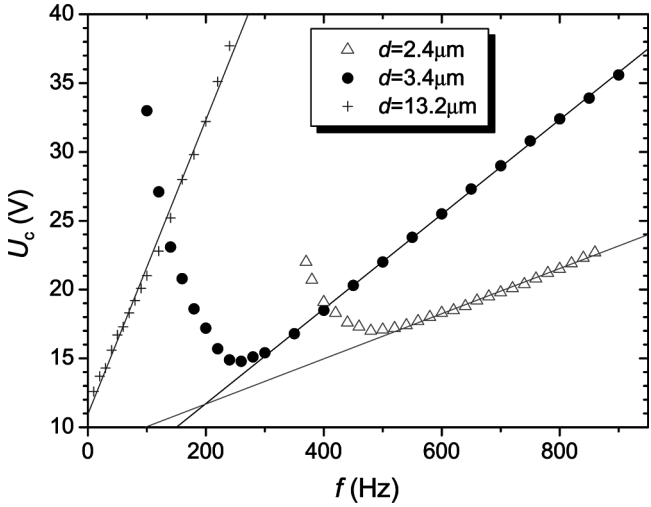

FIGURE 7 ns-EC threshold curves $U_c(f)$ measured in samples of **8**/**7** with different thicknesses d at $T = 76°C$. Solid lines represent linear fit to data.

dielectric s-EC [13], and they indicate the dielectric character of the ns-EC patterns.

CONCLUDING REMARKS

Electroconvection manifests in a flow which is induced by the inhomogeneous (periodic) distribution of space charges, therefore one expects a correlation between EC threshold and these space charges: a more efficient charge separation (in the sense of a stronger generated electric field) leads to lower U_c. The anisotropy of the electrical conductivity σ_a has been established as the reason for the well known Coulomb charge separation mechanism. Flexoelectricity, however, yields another contribution to the charge separation in a periodically deformed state. This flexoelectric effect has usually been neglected in previous studies, though it has emerged from time to time as a possible reason for some unexplained EC features (mostly without a rigorous analysis, however). In the present paper we have reconsidered the role of flexoelectric polarization in electroconvection. We have also extended the scope of experiments and numerical simulations to less studied parameter ranges where flexoelectricity seems to affect the EC characteristics significantly.

The two charge separation mechanisms usually occur concurrently in a nematic. The amount of space charges generated by one or the

Downloaded by [University of California, San Diego] at 14:20 08 August 2012

other mechanism as well as their spatiotemporal distribution may, however, vary depending on material parameters (like σ_a, e_1, e_3) and on experimental conditions (e.g., the driving frequency f). Therefore, either one of the mechanisms can dominate, or when being of the same order they may enhance or reduce each other's effect, which can be either against, or in favor of electroconvection.

The results presented in the paper seem to show examples for each case, which we will label as cases **i.–v.** in the following. We have shown experimentally as well as numerically (within the frame of the "extended" SM) that under the most common EC conditions – $\varepsilon_a < 0$, $\sigma_a > 0$, $d \geq 10\,\mu\text{m}$, $f > 20\,\text{Hz}$, *conductive* regime (case **i.**) – the influence of flexoelectricity on the onset characteristic is negligible, in accordance with former results [2,3]. This indicates the dominance of the Coulomb charge separation mechanism. Reducing the frequency and the thickness (case **ii.**) this dominance seems to cease. The bending down of the $U_c(f)$ curve for $f \to 0$ implies that the flexoelectric space charges have a spatio-temporal distribution which reinforces the effect of the Coulomb charge separation.

The situation in the standard *dielectric* regime in thick cells at high frequencies is similar to case **ii.**, as flexoelectricity decreases the threshold voltage U_c and increases the wave number q_c considerably. In addition, it introduces obliqueness into the roll orientation. The scenario changes again for lower f and d (case **iii.**) where the flexoelectric space charges seem to change their spatio-temporal distribution and compensate the Coulomb ones resulting in the bending up of $U_c(f)$ for low f.

A delicate situation occurs in the class of compounds with $\varepsilon_a < 0$, $\sigma_a < 0$ (case **iv.**) where the sign of σ_a has altered compared to the previously described cases. As a consequence, the Coulomb mechanism induces a stabilizing flow according to the SM, thus alone it would not allow EC. Numerical calculations have, however, proven that the inclusion of flexoelectricity into the SM yields a finite EC threshold voltage even for this parameter combination giving an explanation for the experimentally observed nonstandard EC patterns [7]. This implies that in case **iv.** the flexoelectric contribution has a spatio-temporal distribution that works against the Coulomb one. Moreover, its magnitude has to be larger in order to overcome the stabilizing effects and thus to make the destabilization possible. The bending up of $U_c(f)$ for low f in thin cells (case **v.**) indicates again a reduction and/or a possible spatio-temporal inversion of the flexoelectric space charges. This similarity to case **iii.** supports the idea about the dielectric character of the nonstandard EC instability which has arisen as a conclusion of the extended SM and has recently been confirmed independently by light diffraction measurements [15].

Downloaded by [University of California, San Diego] at 14:20 08 August 2012

The arguments above show that the influence of flexoelectricity on electroconvection is not negligible in general. Its inclusion into the theoretical description is necessary for a proper interpretation of the experimental results in many cases, especially in the dielectric mode (standard or nonstandard) and in the frequency range around and below $1/\tau_d$, where a novel $U_c(f)$ dependence has been detected.

REFERENCES

[1] Kramer, L. & Pesch, W. (1996). Electrohydrodynamic instabilities in nematic liquid crystals. In: *Pattern Formation in Liquid Crystals*, Buka, A. & Kramer, L. (Eds.), Springer-Verlag: New York, Chapter 6, p. 221.

[2] Kramer, L., Bodenschatz, E., Pesch, W., Thom, W., & Zimmermann, W. (1989). *Liq. Cryst.*, *5*, 699.

[3] Madhusudana, N. V. & Raghunathan, V. A. (1989). *Liq. Cryst.*, *5*, 1789.

[4] Meyer, R. B. (1969). *Phys. Rev. Lett.*, *22*, 918.

[5] Petrov, A. G. (2001). Measurements and interpretation of flexoelectricity. In: *Physical Properties of Liquid Crystals: Nematics*, Dunmur, D., Fukuda, A., & Luckhurst, G. (Eds.), INSPEC, The Institution of Electrical Engineers: London, Chapter 5.5, p. 251.

[6] Bodenschatz, E., Zimmermann, W., & Kramer, L. (1988). *J. Phys. France*, *49*, 1875.

[7] Goscianski, M. & Léger, L. (1975). *J. Phys. France*, *36*, 231; Blinov, L. M., Barnik, M. I., Lazareva, V. T., & Trufanov, A. N. (1979). *J. Phys. France*, *40*, 263.

[8] Kochowska, E., Németh, Sz., Pelzl, G., & Buka, Á. (2004). *Phys. Rev. E*, *70*, 011711.

[9] Tóth-Katona, T., Cauquil-Vergnes, A., Éber, N., & Buka, Á. (2007). *Phys. Rev. E*, *75*, 066210.

[10] Kumar, P., Patil, S. N., Hiremath, U. S., & Krishnamurthy, K. S. (2007). *J. Phys. Chem B*, *111*, 8792.

[11] Chistyakov, I. G. & Vistin, L. K. (1974). *Sov. Phys. Crystallogr.*, *19*, 119.

[12] Krekhov, A. P., Pesch, W., Éber, N., Tóth-Katona, T., & Buka, Á. (2008). *Phys. Rev. E*, *77*, 021705.

[13] Tóth-Katona, T., Éber, N., Buka, Á., & Krekhov, A. P. (2008). *Phys. Rev. E*, *78*, 036306.

[14] Vistin, L. K. (1970). *Kristallografiya*, *15*, 594; Bobylev, Yu. P. & Pikin, S. A. (1977). *Sov. Phys. JETP*, *45*, 195.

[15] Tóth-Katona, T., Éber, N., & Buka, Á. (unpublished).

Downloaded by [University of California, San Diego] at 14:20 08 August 2012